JOURNAL OF ELECTROMAGNETIC ENGINEERING AND SCIENCE, VOL. 15, NO. 1, 1~5, JAN. 2015

http://dx.doi.org/10.5515/JKIEES.2015.15.1.1
ISSN 2234-8395 (Online) · ISSN 2234-8409 (Print)

Review of the Hidden Rays of Diffraction

(Invited Paper)

Se-Yun Kim*

Abstract

A high-frequency analysis technique, called the hidden rays of diffraction (HRD), is reviewed in this paper. The physical optics and the rigorous diffraction coefficients of a perfectly conducting wedge illuminated by a plane wave are compared. The physical existence of hidden rays on the shadow boundary is explained in view of the geometric theory of diffraction (GTD). In particular, a systematic tracing of hidden rays and its visualization are precisely described by introducing the concept of the supplementary boundary. The physical meaning of the null-field condition in the complementary region is also explained.

Key Words: Diffraction, Edge, Physical Optics, Ray-Tracing, Wedge.

I. INTRODUCTION

The geometrical theory of diffraction (GTD) [1] has played a prominent role in high-frequency analysis of electromagnetic scattering and diffraction. The asymptotic diffraction coefficients of a perfectly conducting wedge, which was rigorously derived more than one century ago, laid the foundation of the GTD technique. Until now, however, there have been no rigorous diffraction coefficients of penetrable wedges. As a detour, we performed the physical optics (PO) approximation on the lit boundary of a dielectric wedge [2]. Next, the correction to the PO diffraction coefficients was implemented by numerically calculating the non-uniform currents on its lit and shadow boundaries [3, 4].

Recently, the finite difference time domain (FDTD) method has been employed to calculate the diffraction coefficients of penetrable wedges numerically without any analytical treatment [5]. However, the fully numerical approach could not provide any physical understanding of the inherent features in the wedge diffraction. On the other hand, a systematic tracing of the geometrical rays, which are reflected and refracted on the shadow boundary of a penetrable wedge, was presented. This technique, called the hidden rays of diffraction (HRD) [6], provided more accurate diffraction coefficients of some canonical penetrable wedges [7−9] than the conventional PO solutions. In this paper, the physical background and fundamental issues of the HRD technique are reviewed in detail by reinterpreting the diffraction coefficients of a perfectly conducting wedge.

II. PHYSICAL BACKGROUND

For a wedge illuminated by a plane wave, its geometrical optics (GO) field is expressed by a finite sum of ordinary rays, which are incident, reflected, and refracted on the lit boundary. Here the term 'ray' denotes a plane wave with the same amplitude and propagation angle. In contrast, its PO solution is given by an integral of the diffraction coefficients along the Sommerfeld's path P [10]. The PO diffraction coefficients consist of the same number of cotangent functions as the ordinary rays. In asymptotic integration, the P path is deformed into the steepest decent path (SDP) [10] and the closed P-SDP path.

Manuscript received December 12, 2014 ; January 9, 2015 ; Accepted January 13, 2015. (ID No. 20141212-03J)
Imaging Media Research Center, Korea Institute of Science and Technology, Seoul, Korea.
*Corresponding Author: Se-Yun Kim (e-mail: ksy@imrc.kist.re.kr)

Then the integrations of the PO diffraction coefficients along the contour P-SDP and the SDP are equal to the GO term and the edge-diffracted field, respectively. Therefore, there is one-to-one correspondence between the ordinary rays of its GO field and the diffraction coefficients of its PO field [2, 6]. It causes the PO diffraction coefficients to be constructed routinely only from the conventional ray-tracing data.

In general, however, the PO field cannot satisfy the boundary condition at the wedge interface and the edge condition at the wedge tip. The GO field is the perfect first term of the asymptotic series solution in high frequency. The error of the PO field is then generated by the PO diffraction coefficients as the imperfect second term. From the traditional point of view, the error of the PO diffraction coefficients could be corrected by adding the non-uniform currents on wedge interfaces. In particular, both non-uniform currents on the lit and shadow boundaries are required for the same physical reason and are expressed in the same mathematical form.

The starting line of the HRD technique was the comparison between the PO and exact diffraction coefficients of a perfectly conducting wedge. Consider an E-polarized plane wave incident only on its lit boundary at $\theta = \theta_c$, as shown in Fig. 1. In this case, the PO solution $u^{(PO)}(\rho,\theta)$ and exact total field $u^{(ex)}(\rho,\theta)$ were expressed in the same asymptotic integral form [10] as

$$\begin{Bmatrix} u^{(PO)}(\rho,\theta) \\ u^{(ex)}(\rho,\theta) \end{Bmatrix} = \frac{1}{2\pi i}\int_P dw \begin{Bmatrix} f_1(w) \\ p_1(w) \end{Bmatrix} e^{ik_0\rho\cos(w-\theta)} = u^{(GO)}(\rho,\theta) + \frac{1}{2\pi i}\int_{SDP} dw \begin{Bmatrix} f_1(w) \\ p_1(w) \end{Bmatrix} e^{ik_0\rho\cos(w-\theta)}. \quad (1)$$

In Eq. (1), the GO field $u^{(GO)}(\rho,\theta)$ is well known as

$$u^{(GO)}(\rho,\theta) = W(\theta_{i.c},\theta_c)e^{ik_0\rho\cos(\theta-\theta_{i.c})} + W(\theta_{r.c},\theta_c)R_c e^{ik_0\rho\cos(\theta-\theta_{r.c})}, \quad (2)$$

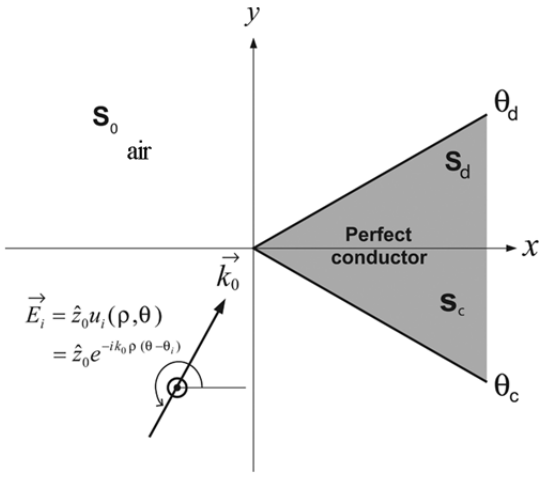

Fig. 1. A perfectly conducting wedge illuminated by an E-polarized plane wave for $\theta_i > \theta_d + \pi$.

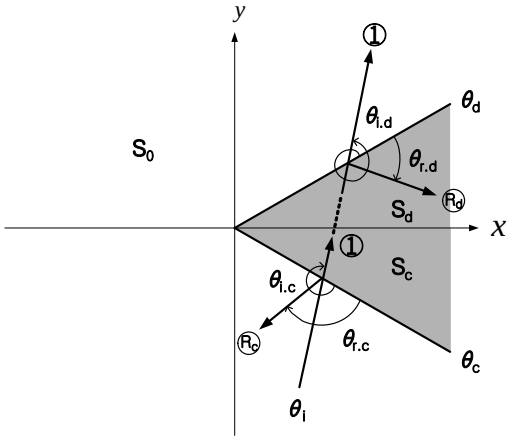

Fig. 2. The propagation angles of the ordinary rays on the lit boundary and the hidden rays on the shadow boundary for $\theta_i > \theta_d + \pi$.

where the angular window function W is defined by

$$W(\theta_a,\theta_b) = \begin{cases} 1, & for\ \theta_a \le \theta \le \theta_b \\ 0, & elsewhere \end{cases}. \quad (3)$$

The PO diffraction coefficients $f_1(w)$ are written by

$$f_1(w) = -\frac{1}{2}\left[\cot\left(\frac{w-\theta_{i.c}}{2}\right) + R_c\cot\left(\frac{w-\theta_{r.c}}{2}\right)\right]. \quad (4)$$

The exact diffraction coefficients $p_1(w)$ are given by

$$p_1(w) = p_{1c}(w) + p_{1d}(w), \quad (5)$$

where

$$p_{1c}(w) = -\frac{1}{2\nu_\infty}\left[\cot\left(\frac{w-\theta_{i.c}}{2\nu_\infty}\right) + R_c\cot\left(\frac{w-\theta_{r.c}}{2\nu_\infty}\right)\right], \quad (6a)$$

$$p_{1d}(w) = \frac{1}{2\nu_\infty}\left[\cot\left(\frac{w-\theta_{i.d}}{2\nu_\infty}\right) + R_d\cot\left(\frac{w-\theta_{r.d}}{2\nu_\infty}\right)\right]. \quad (6b)$$

Each pole of the cotangent functions in Eqs. (4) and (6) denotes the propagation angle of the corresponding ray, as shown in Fig. 2. It should be noted that the propagation angle of a ray in Fig. 2 is accounted for by the sum of the angle of its reference line and the variation angle of its angular arrow. When the direction of the angular arrow is counterclockwise (clockwise), the variation angle is considered as a positive (negative) value. Both reflection amplitudes R_c and R_d are equal to -1 in this case.

Two cotangent functions in Eq. (6a) can be constructed from the PO diffraction coefficients in Eq. (4) only if the angular period of the cotangent functions is adjusted from 2π to $2\pi\nu_\infty$, where ν_∞ is obtained from the edge condition [11] at the wedge tip as

$$\nu_\infty = \frac{(\theta_c - \theta_d)}{\pi}. \quad (7)$$

Considering the one-to-one correspondence between the ordinary rays and the PO diffraction coefficients, one may routinely construct two cotangent functions in Eq. (6a) only from the ordinary ray-tracing data and the edge condition. This leads us to conclude that the ordinary rays on the lit boundary generate the first two cotangent functions in Eq. (5).

In Fig. 1, the incident field cannot reach the shadow boundary at $\theta = \theta_d$. Therefore, no actual reflection occurs on the shadow boundary. However, the exact solution in Eq. (5) consists of four cotangent functions, among which the last two should directly relate to the reflection on the shadow boundary. In a pure mathematical way, Fig. 2 illustrates the propagation angles and amplitudes of the incident and reflected rays on the $\theta = \theta_d$ boundary. According to traditional optics, however, there is no systematic way to trace the geometrical rays on the shadow boundary. Therefore, it is impossible to see these rays in the physical region. Thus, these extraordinary rays are called hidden rays [5].

III. Fundamental Issues

Several arguing points are posed vis-a-vis the so-called hidden rays. The first issue is how to infer the physical existence of the hidden rays on the shadow boundary from the mathematical expression in Eq. (6b). In case of Fig. 1, not only the lit boundary at $\theta = \theta_c$ but also its edge as the end-point of the lit boundary are illuminated simultaneously by the incident plane wave. At first, the ordinary rays on the lit boundary provide the GO field. According to the GTD, the diffracted field in a wedge may be interpreted as the field radiated from the induced currents at its edge. The GO field at the edge as the end-point of the lit boundary then generates the corresponding edge-diffracted field, as shown in Eq. (6a).

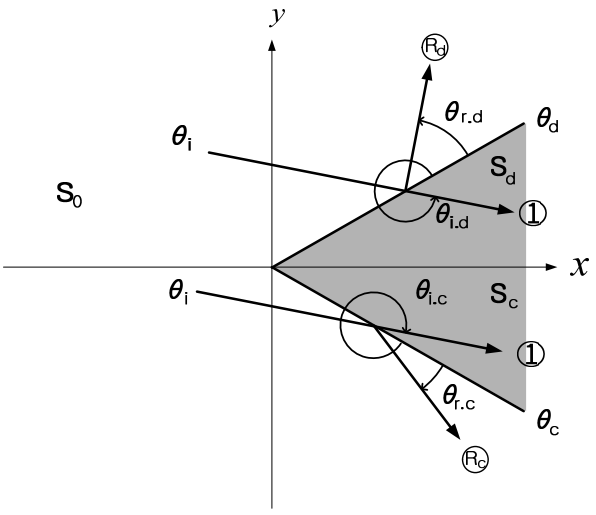

Fig. 3. The propagation angles of the ordinary rays on both boundaries for $\theta_d < \theta_i < \theta_c$.

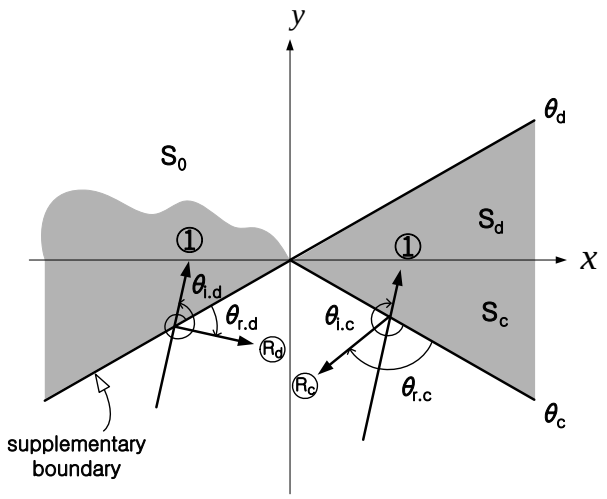

Fig. 4. A perfectly conducting wedge illuminated by an E-polarized plane wave for $\theta_i > \theta_d + \pi$.

Naturally, the incident wave in Fig. 1 cannot reach the shadow boundary at $\theta = \theta_d$. Thus, no ordinary rays on the shadow boundary cause the corresponding GO field to be zero. However, the edge as the end-point of the shadow boundary is illuminated by the incident plane wave. This implies that the edge-diffracted field radiated from the induced currents at the edge as the end-point of the shadow boundary cannot become zero, as shown in Eq. (6b). In a reverse sense, one may guess that the diffraction coefficients in Eq. (6b) are also constructed from the hidden rays one by one.

The above inference leads us to argue such the second issue as where the hidden rays exist. The poles of the two cotangent functions in Eq. (6b), which are directly equal to the propagation angles of the two hidden rays in Fig. 2, are well known as

$$\begin{cases} \theta_{i.d} = \theta_i + \pi \\ \theta_{r.d} = 2(\theta_d + \pi) - \theta_{i.d} \end{cases}. \tag{8}$$

One cannot intuitively divine the physical meaning of the angles in Eq. (8). As a detour, consider that both boundaries of the wedge in Fig. 1 are illuminated by the incident plane wave for $\theta_d < \theta_i < \theta_c$. The ordinary ray-tracing result in this case is shown in Fig. 3. It is an interesting feature that the propagation angles of two ordinary rays on the $\theta = \theta_d$ boundary are also expressed by Eq. (8). In other words, hidden rays on a shadow boundary can be traced according to the same ray-tracing rule when the shadow boundary is illuminated by the plane wave with a different incident angle.

The third issue may be how to easily implement the visualization of the hidden ray tracing on the shadow boundary. As suggested in [6], a supplementary boundary was introduced by rotating the shadow boundary by 180° toward the air region.

Then, as shown in Fig. 4, the incident plane wave can be incident on the supplementary boundary corresponding to the shadow boundary. It should be noted that the angle of the supplementary boundary is not $\theta_d + \pi$ but θ_d because its introduction is only for the visualization of the hidden ray tracing.

The last issue is strongly related to the angular period of the diffraction coefficients. The PO cotangent functions in Eq. (4) have the angular period 2π. In contrast, the angular period of the exact diffraction coefficients increases up to $2\pi\nu_\infty$ because according to Eq. (7), ν_∞ is a positive real value larger than 1 but less than 2. The induced currents on the lit boundary then generate the diffraction coefficients $p_{1c}(w)$ in Eq. (6a), as shown in Fig. 5. Because the angular period of $p_{1c}(w)$ is $2\pi\nu_\infty$, its angular distribution range should be down to $\theta_c - 2\pi\nu_\infty$. On the other hand, the diffraction coefficients $p_{1d}(w)$ generated from the induced currents on the shadow boundary should be distributed up to $\theta_d + 2\pi\nu_\infty$.

The physical air region S_0 in Fig. 1 is $[\theta_d, \theta_c]$. Based on the formulation of dual integral equations [2], the concept of the complementary air region was introduced [6]. The complementary air region $S_c^{(0)}$ is defined in the angular range of $(\theta_c, 2\pi]$ or $(\theta_c - 2\pi, 0]$ where the original conductor is replaced by air. In the same manner, $S_d^{(0)}$ denotes the other complementary air region in $[0, \theta_d)$ or $[2\pi, \theta_d + 2\pi)$. For convenience, the physical and complementary regions are limited to $[0, 2\pi]$. The exact diffraction coefficients are then expressed in different forms as

$$p_1(w) = \begin{cases} p_{1c}(w) + p_{1d}(w + 2\pi) = 0, & in \quad 0 \le w < \theta_d \\ p_{1c}(w) + p_{1d}(w) \quad , & in \quad \theta_d \le w \le \theta_c \\ p_{1c}(w - 2\pi) + p_{1d}(w) = 0, & in \quad \theta_c < w \le 2\pi \,. \end{cases} \tag{9}$$

In particular, one may easily prove that the exact diffraction coefficients in two complementary air regions of $[0, \theta_d)$ and $(\theta_c, 2\pi]$ become zero, as shown in Eq. (9). This property is called the null-field condition in the complementary region.

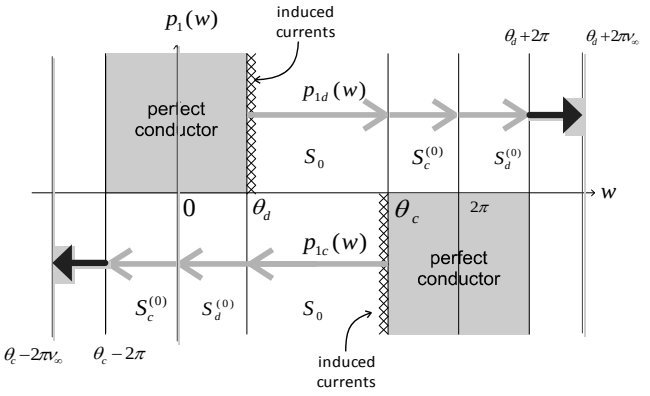

Fig. 5. Angular distribution of the common physical air region S_0 in Fig. 1 and two complementary air regions $S_c^{(0)}$ and $S_d^{(0)}$.

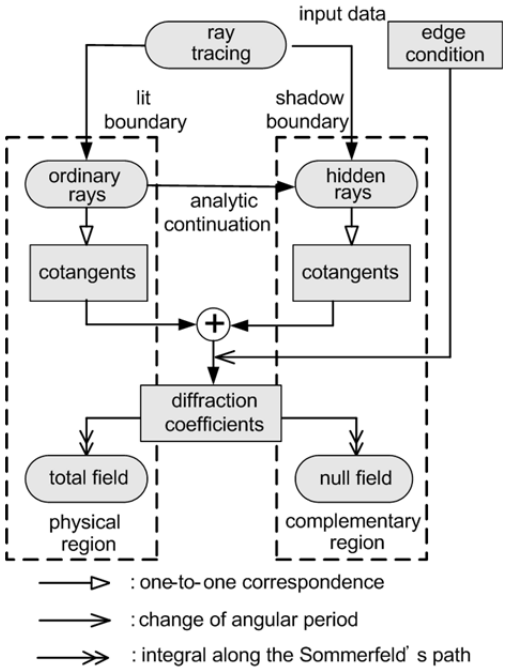

Fig. 6. Standard procedure of the hidden rays of diffraction (HRD) technique.

This null-field condition has been used as a criterion to check the accuracy of the HRD solution to a wedge [6].

All the above properties formed a framework for implementing the HRD technique to solve a penetrable wedge problem. The standard procedure of the HRD technique, as illustrated well in Fig. 6, has provided more accurate diffraction coefficients of some canonical wedges [6−9].

IV. CONCLUSION

In this paper, the physical existence and tracing rule of the hidden rays reflected and refracted on the shadow boundary are explained in detail by comparing the PO and the exact diffraction coefficients of a perfectly conducting wedge. The visualization of the hidden ray tracing on the shadow boundary is easily implemented by introducing its supplementary boundary. The null-field condition in the complementary region is also explained in detail. Compared to the physical theory of diffraction (PTD) [12], the HRD technique provides not only a pure analytic form of the diffraction coefficients of some canonical wedges but also a new aspect of the physical understanding of diffraction by a wedge. It is expected that this brief review will be helpful in applying the HRD technique to a wide range of diffraction problems.

This research was supported by the Korea Institute of Science and Technology Institutional Program (No. 2E-24790).

REFERENCES

[1] J. B. Keller, "Geometrical theory of diffraction," *Journal of Optical Society of America*, vol. 52, no. 2, pp. 116−130, 1962.

[2] S. Y. Kim, J. W. Ra, and S. Y. Shin, "Diffraction by an arbitrary-angled dielectric wedge. Part I: Physical optics approximation," *IEEE Transactions on Antennas and Propagation*, vol. 39, no. 9, pp. 1272−1281, Sep. 1991.

[3] S. -Y. Kim, J. W. Ra, and S. Y. Shin, "Diffraction by an arbitrary-angled dielectric wedge. Part II: Correction to physical optics solution," *IEEE Transactions on Antennas and Propagation*, vol. 39, no. 9, pp. 1282−1292, Sep. 1991.

[4] S. Y. Kim, "Diffraction coefficients and field patterns of obtuse angle dielectric wedge illuminated by E-polarized plane wave," *IEEE Transactions on Antennas and Propagation*, vol. 40, no. 11, pp. 1427−1431, Nov. 1992.

[5] G. Stratis, V. Anantha, and A. Taflove, "Numerical calculation of diffraction coefficients of generic conducting and dielectric wedges using FDTD," *IEEE Transactions on Antennas and Propagation*, vol. 45, no. 10, pp. 1525−1529, Oct. 1997.

[6] S. Y. Kim, "Hidden rays of diffraction," *IEEE Transactions on Antennas and Propagation*, vol. 55, no. 3, pp. 892−906, Mar. 2007.

[7] S. Y. Kim, "Hidden rays of diffraction for dielectric wedge," *Radio Science*, vol. 42, no. 6, pp. 1−11, 2007.

[8] S. Y. Kim, "Hidden rays of diffraction for a composite wedge composed of a perfect conductor and a lossy dielectric," *IEICE Transactions on Communication*, vol. 94B, no. 2, pp. 484−490, Feb. 2011.

[9] S. Y. Kim, "H-polarized diffraction coefficients of a composite wedge composed of a perfect conductor and a lossy dielectric," *IEEE Transactions on Antennas and Propagation*, vol. 60, no. 4, pp. 2126−2128, Apr. 2012.

[10] L. B. Felsen and N. Marcuvitz, *Radiation and Scattering of Waves.* Englewood Cliffs, NJ: Prentice-Hall, 1973.

[11] J. Meixner, "The behavior of electromagnetic fields at edges," *IEEE Transactions on Antennas and Propagation*, vol. 20, no. 4, pp. 442−446, Jul. 1972.

[12] P. IA. Ufimtsev, *Fundamentals of the Physical Theory of Diffraction.* Hoboken, NJ: Wiley, 2007.

Se-Yun Kim

received his B.S. degree from Seoul National University, Seoul, Korea in 1978 and his M.S. and Ph.D. degrees from the Korea Advanced Institute of Science and Technology, Seoul, Korea in 1980 and 1984, respectively, all in electrical engineering. He was Postdoctoral Fellow from 1984 to 1986 at the Korea Advanced Institute of Science and Technology. In 1986, he joined the Korea Institute of Science and Technology, Seoul, Korea, as a Senior Researcher. He is currently a Principal Researcher at the Korea Institute of Science and Technology. His research interests include electromagnetic scattering, microwave imaging and geophysical probing. Dr. Kim received the Academic Achievement Award from the Institute of Electronics and Information Engineers in 1988, the Order of National Security Merit from the Korean Government in 1990, and the Paper Award at the ISAP'2007, Niigata, Japan. He has been the Man of National Merit since 1991.